

Contact Friction Analysis of Silicon Material

*Jeng-Haur Horng^a, Chin-Chung Wei^b, Yang-Yuan Chen^c, Chan-Hui Huang^d

Abstract—With the scientific and technological accurate trend with diminish gradually of orientation, it has become increasingly important to study the surface phenomena. When surface touch each other, contact friction is predominantly made at the summits of surface roughness and particle. The particle effect and its manifestation in friction still attracts considerable debate as to its likely causes. Analysis had been conducted to study the important contribution that the formation of friction debris can have on the progression of friction. Based on the contact mechanics and friction theory, this work establishes a new three-body friction model with considering the surface friction and deformation friction of particles. It is proposed in order to understand the effects of particles between surfaces on contact characteristics for rough surface with different particle size.

The results show that the particle size and plasticity index dominates the friction value for low mean separation between rough surfaces. Beyond the critical value of mean separation, the important factor in affecting total friction value is surface friction partition of total friction. The critical value have the sequence for the different particle sizes: $(d/\sigma)_{c_{n=500}} > (d/\sigma)_{c_{x=100}} > (d/\sigma)_{c_{x=20}}$ at the same ratio x/Rq . The larger the wear particle size, the higher friction value and critical separation value for silicon under the same roughness parameters.

Index Terms—adhesion, friction, wear, particle, three-body microcontact

I. INTRODUCTION

Accurate prediction of friction coefficient is essential for many modern tribological applications such as head-disk interface in magnetic storage, microelectromechanical systems, seals, and clutches to name a few. The mechanisms of friction between two solids have been extensively studied. However, a complete explanation of the phenomenon is still missing. The experimental work by Amontons in 1699 and Coulomb in 1785 showed that the proportionality of the force opposing relative motion to the force holding the bodies together seemed to be constant over a range of conditions. A significant number of experiments under different conditions have been performed, and this friction model is usually applicable only to a specific interface [1-4]. Blau [5] indicated that friction coefficient is relatively easy to determine in a laboratory, but the fundamental origins of

sliding resistance are not so clear. Tabor [6] pointed out that the true contact area and intermolecular forces of contact between rough surfaces are important elements in the friction of dry solids.

In 1988, Chang et al. [7] extended the CEB contact model to calculate the static friction coefficient (CEB friction model). However, the CEB friction model underestimates the friction coefficient because it neglects the ability of elastic-plastic deformed asperities to resist additional tangential loading. This problem was resolved by Kogut and Etsion [8] (KE friction model). Polycarpou and Etsion [9] modified the CEB friction model to include the presence of sub-boundary lubrication. Chang and Zhang [10] presents a mathematical model for frictional elastic-plastic sphere-on-flat contacts to consider the sliding incipient effect. In practical motion devices, wear debris or contaminant particles at the interface are common. However few studies have been conducted a three-body microcontact model that includes. Recently, Zhang and Bogy [11], Shen and Bogy, [12,13] and, Stachowiak, [14] discussed the effect of particles in head disk interference on wear, contact force, and temperature rise. In this work, a three-body microcontact model of rough surfaces [15] is used to describe the contact characteristics. A modified elastic-plastic adhesion model for a metallic deformable sphere pressed by a rigid flat is used to calculate the adhesive force [16]. In this paper, Contact friction for rough surfaces with particles is proposed to understand the effects of particles between surfaces on silicon material.

II. ANALYSIS

1. Microcontact Model

In the contact model, we made the following assumptions: 1. All surface asperities are far apart and there is no interaction between them. 2. There is no bulk deformation, only the surface asperities deform during contact. 3. The diameter of spherical particles is D and much harder than the upper and lower contact surfaces, which deform plastically during contact with particles. 4. Slopes of surface asperities are negligibly small. Figure 1 shows the geometry of the three contacting bodies : surface 1, surface 2, and the particles. Here, z and d denote the asperity height and separation of surfaces, respectively.

^aDepartment of Power Mechanical Engineering, National Formosa University, Taiwan, ROC

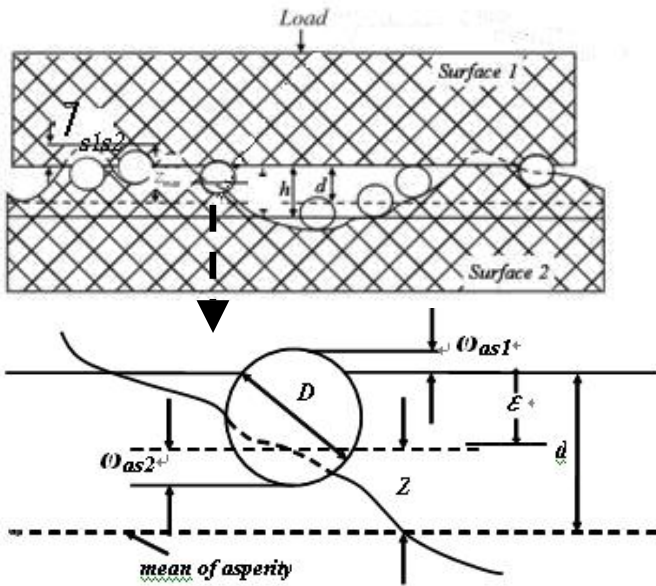


Fig. 1 Geometry of three contacting bodies

According to the paper [17], the tree-body microcontact model becomes:

$$F_{total} = F_{as1} + F_{s1s2-as1} = \frac{\pi H_{s1} H_{s2} \eta_a A_n}{H_{s1} + H_{s2}} \left[\frac{9\pi^2}{4} \left(\frac{H_{s1}^2}{E_{as1}^2} + \frac{H_{s2}^2}{E_{s1s2}^2} \right) \int_{d-h_e}^d x^2 \phi_a(x) dx + \int_d^{x_{max}} x^2 \phi_a(x) dx \right] + \left(1 - \frac{\pi H_{s1} \eta_a}{H_{s1} + H_{s2}} \int_{x_{min}}^{x_{max}} x^2 \phi_a(x) dx \right) \cdot F_{s1s2} \quad (1)$$

$$A_{total} = A_{as1} + A_{s1s2-as1} = \frac{\pi H_{s2} \eta_a A_n}{H_{s2} + H_{s1}} \left[\frac{9\pi^2}{4} \left(\frac{H_{s1}^2}{E_{as1}^2} + \frac{H_{s2}^2}{E_{s1s2}^2} \right) \int_{d-h_e}^d x^2 \phi_a(x) dx + \int_d^{x_{max}} x^2 \phi_a(x) dx + A_{s1s2} \right] \cdot \left\{ 1 - \frac{\pi H_{s1} \eta_a}{H_{us1} + H_{ds2}} \int_d^{x_{max}} x^2 \phi_a(x) dx \right\} \quad (2)$$

where A_{s1s2} is the real total contact area of the two-body microcontact models. The total contact areas A_i , and the total contact load F_i of the three bodies can be obtained from Eq. (1) and (2).

2. Adhesion

The MDT adhesion model was modified by Kogut and Etsion [16]. Their model is much more accurate than the previous one, which relied on a certain approximation the local separation outside the contact area above the critical interference. The simple analytical expression is:

2.1 Elastic contact

The dimensionless adhesion force in the elastic contact regime, $\omega/\omega_c < 1$, yields:

$$\frac{F_s}{F_{s0}} = 0.979 \left(\frac{\varepsilon}{\omega_c} \right)^{-0.29} \left(\frac{\omega}{\omega_c} \right)^{0.298} \quad (3)$$

for $0.005 \leq \varepsilon/\omega_c \leq 0.5$,

$$\frac{F_s}{F_{s0}} = 1.001 + \frac{0.192 \omega/\omega_c}{\varepsilon/\omega_c} \quad (4)$$

for $0.5 \leq \varepsilon/\omega_c \leq 100$

Where ε is the intermolecular distance, which is about 0.3nm~0.5nm.

2.2 Elastic-plastic contact

The dimensionless adhesion force, F_s/F_{s0} , in the elastic-plastic contact regime, $1 \leq \omega/\omega_c \leq 110$, can be calculated for the larger sphere radii $0.005 \leq \omega/\omega_c \leq 0.5$:

$$\frac{\bar{F}_s}{F_{s0}} = 0.792 \left(\frac{\varepsilon}{\omega_c} \right)^{-0.321} \left(\frac{\omega}{\omega_c} \right)^{0.356} \quad (5)$$

for $1 \leq \omega/\omega_c \leq 6$,

$$\frac{\bar{F}_s}{F_{s0}} = 1.193 \left(\frac{\varepsilon}{\omega_c} \right)^{-0.322} \left(\frac{\omega}{\omega_c} \right)^{0.093} \quad (6)$$

for $6 \leq \omega/\omega_c \leq 110$, and for the smaller sphere radii $0.5 < \omega/\omega_c \leq 110$:

$$\frac{\bar{F}_s}{F_{s0}} = 0.961 + \frac{0.157}{\omega/\omega_c} + \frac{0.261 \ln(\omega/\omega_c)}{\varepsilon/\omega_c} \quad (7)$$

for $1 \leq \omega/\omega_c \leq 6$

$$\frac{\bar{F}_s}{F_{s0}} = 1.756 - \left(0.516 - \frac{0.303}{\varepsilon/\omega_c} \right) \ln \frac{\omega}{\omega_c} + 0.052 \left(\ln \frac{\omega}{\omega_c} \right)^2 \quad (8)$$

for $6 \leq \omega/\omega_c \leq 110$

3. Friction

Our friction analysis model is based on the analyses of Komvopoulos et al. [18] and Bhushan et al.[19-20]. The friction is expressed as the sum of four components: surface asperity deformation (Q_d), plowing deformation by particles entrapped between contact surface (Q_a), adhesive friction (Q_s), and ratchet friction (Q_r) at the contact region. The total friction force and friction components become:

$$Q = Q_d + Q_a + Q_s + Q_r = A_r \tau_a + A_{s1s2-s1a} \tau_{s1s2} + A_{s1a} \tau_{s1a} + A_{s1s2-s1a} \tau_{s1s2} \times \tan^2 \theta \quad (9)$$

where A_r , $A_{s1s2-s1a}$, and A_{s1a} are the real areas of contact during adhesion, two surface deformation, and particle-surface1 deformation, respectively. They are calculated from Eq(18). τ_a , τ_{s1s2} , and τ_{s1a} , are the shear strengths during adhesion, two surface deformation, and particle-surface deformation [20], respectively.

III RESULTS AND DISCUSSION

The material used in the analysis was nickel; its material properties are listed in Table 1. Figure 2 shows the total friction versus dimensionless mean separation at various particle sizes for $\Psi=1.5$, and $R_q=100\text{nm}$. The total friction coefficient decreases with increasing mean separation (d/σ) for different particle sizes. For small values of d/σ , large particle makes more large friction coefficient than that of small particle size at the same mean separation. However, for large values of d/σ , they have the almost same value of friction coefficient for different particle sizes.

Table1 Material properties of Silicon

Property	Value
Surface Free Energy, $\Delta\gamma$ (J/m ²)	0.1
Upper Specimen Hardness, H (GPa)	12
Lower Specimen Hardness, H (GPa)	12
Upper Specimen Young's modulus, E (GPa)	190
Lower Specimen Young's modulus, E (GPa)	190
Particle Young's modulus, E (GPa)	190
Upper Specimen Poisson ratio, ν	0.29
Lower Specimen Poisson ratio, ν	0.29
Nominal Contact Area, A_n (m ²)	506.7×10^{-9}

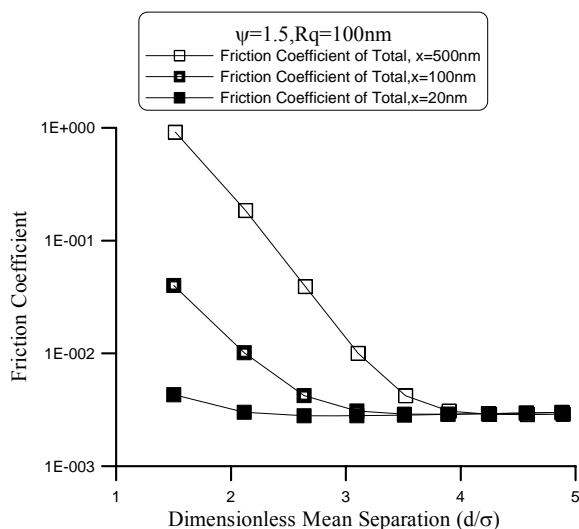


Figure 2. Total friction coefficient varying with dimensionless mean separation for various particle sizes.

Figure 3(a) shows the total, surface, and particle friction coefficients versus dimensionless mean separation for $\Psi=1.5$, $R_q=100\text{nm}$, and $x=100\text{nm}$. The total friction coefficient decreases with increasing mean separation (d/σ) under the same contact and operating conditions, as shown in Figure 2. For small values of d/σ , the dominant factor in total friction coefficient is particle deformation friction. For large values of d/σ , surface friction is the main factor that affects the total friction coefficient above the critical separation $d/\sigma = 3.4$. Comparing Figure 2 with Figure 3(a) it can be seen that the surface friction force increases with decreasing mean

separation (d/σ). However, its increase rate was lower than that of the external force rate and particle friction force. This is the reason causing the surface friction to gradually decreasing with increasing mean separation. It is interesting to note that, for the three body contact situation, a smaller particle size has a smaller particle friction coefficient than that of a large particle size at fixed dimensionless separation, as shown in Figure 3(b) and 3(c). The critical values of separation are 1.31 ($x=20\text{nm}$), 2.44 ($x=100\text{nm}$), and 3.4 ($x=500\text{nm}$). The sequence for the different particle size is: $(d/\sigma)_{C_{x=500}} > (d/\sigma)_{C_{x=100}} > (d/\sigma)_{C_{x=20}}$ at the same ratio x/R_q .

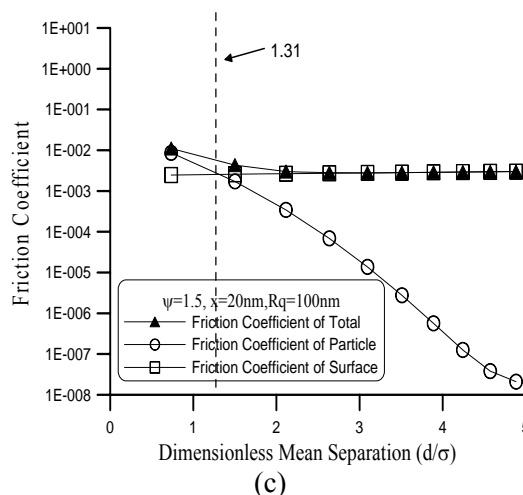
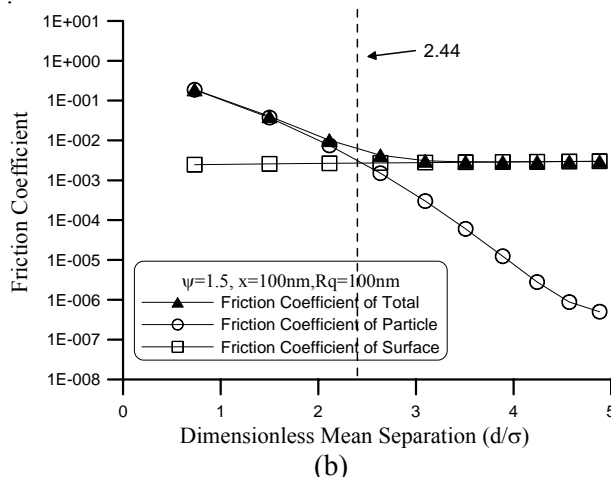
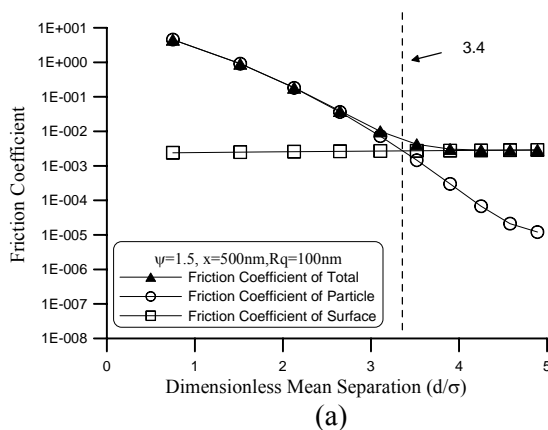


Figure 3. Total friction coefficient varying with dimensionless mean separation for various particle sizes; (a) $x=500\text{nm}$. (b) $x=100\text{nm}$. (c) $x=20\text{nm}$.

In order to examine the main affecting factor of surface friction coefficient, the all components of the surface friction coefficient were performed for the different dimensionless separations, as shown Figure 4. As the dimensionless separation increased, the deformation friction coefficient became most important for all surface frictions. Figure 5 shows the effects of the plowing deformation regime of particles on the particle friction coefficient. It indicates that the particle deformation friction is mainly affected by the plastic deformation friction coefficient of wear particles. The agreement between theoretical friction and experiments by Komvopoulos et al. [18] was good.

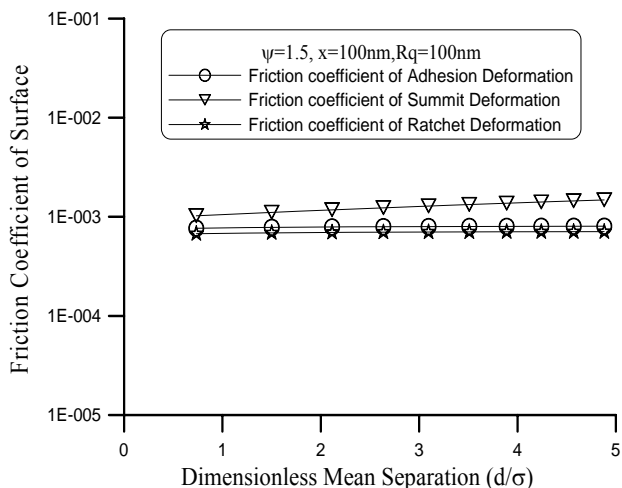


Figure 4. Surface friction coefficient components varying with dimension mean separation for $x=100$ nm.

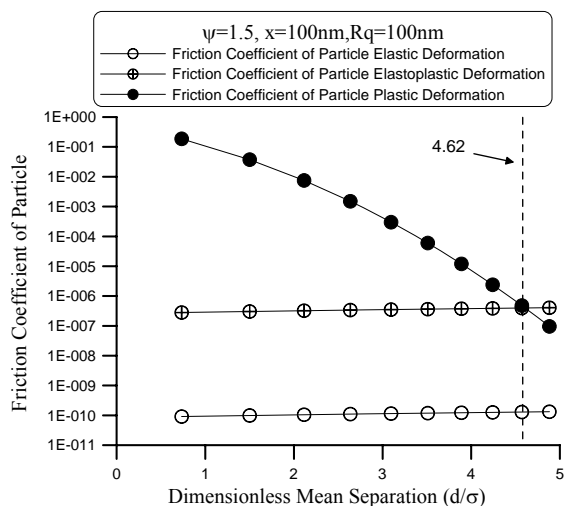


Figure 5. Particles friction coefficient components varying with dimensionless mean separation for $x=100$ nm.

[3]H. Nolle, and R. S. H. Richardson, Static Friction coefficient for Mechanical and Structural Joints, wear Vol. 28, 1974, pp. 1-13.
 [4] D. Buckley, The Metal-to Metal Interface and Its Effect on Adhesion and Friction, J. of Colloid and Interface Science, Vol. 58, 1977, pp. 36-53.
 [5] P. J. Blau, The Significance and Use of the Friction coefficient, Tribol. Int., Vol. 34, 2001, pp. 585-591.
 [6] D. Tabor, Friction----The Present State of Our Understanding, ASME J. Lubr. Technol., Vol.103, 1981, pp. 169-179.
 [7] W. R. Chang, and I. Etsion, and D. B. Bogy, Static Friction Coefficient Model for Metallic Rough Surfaces, ASME Journal of Tribology, Vol. 110, 1988, pp. 57-63.
 [8] L. Jogut, and I. Etsion, A Static Friction Model for Elastic-Plastic Contacting Rough Surface, ASME Vol. 126, 2004, pp. 34-40
 [9] A. A. Polycarpou, and I. Etsion, Static Friction of Contacting Real Surfaces in the Presence of Sub-Boundary Lubrication, ASME, J. Tribol., Vol. 120, 1998, pp. 296-303.
 [10] L. Chang, and H. Zhang, A Mathematical Model for Frictional Elastic-Plastic Sphere-on-Flat Contacts at Sliding Incipient, ASME Vol. 74, 2007, pp.100-106.
 [11] S. Zhand, and D.B.Bogy, Slider Designs for controlling contamination, ASME J. Tribol., Vol. 119, 1997, pp.537-540.
 [12] X.-J. Shen, and D.B. Bogy, Particle Flow and Contamination in Slider Air Bearings for Hard Disk Drives, ASME J. Tribol., Vol. 125, 2002, pp. 358-363.
 [13] X.-J. Shen, and D.B. Bogy, Contact Force and Frictional Heating due to "Large" Particles in the Head Disk Interface, ASME J. Tribol., Vol. 130 2008, pp.011015-1~011015-7
 [14] G. B. Stachowiak, and G. W. Stachowiak, The Effects of Particle Characteristics on Three-Body Abrasive Wear, Wear, Vol. 249, 2001, pp. 201-207.
 [15] J. H. Horng, J. S. Lee, D. C. Du, Three-Body Microcontact Model of Rough Surfaces and Its Application on Polishing of Wafer, Material Science Forum, Vols. 505-507, 2006, pp.445-450.
 [16]L. Hogut, and I. Etsion, Adhesion in elastic-plastic spherical microcontact, Journal of Colloid and Interface Science Vol. 261, 2003, pp. 372-378.
 [17]J.H Horng, J. S. Lee, D. C. Du, Three-Body Microcontact Model of Rough Surface Surfaces and Its Application on Polishing of Wafer, Material Science Forum, 2006, pp. 507-513.
 [18] K. Komvopoulos, N. Saka, and N.P. Suh, Plowing Friction in Dry and Lubricated Metal Sliding, ASME Journal of Tribology, Vol. 108, 1986, pp. 301-313.
 [19]B. Bhushan and M.Nosonovsky, Scale Effects in Friction Using Strain Gradient Plasticity and Dislocation-Assisted Sliding (Microslip), Acta Mater., Vol. 51, 2003, pp. 4331-4345.
 [20]B. Bhushan, and M. Nosonovsky, Comprehensive Model for Scale Effects in Friction Due to Adhesion and Two- and Three-Body Deformation (Plowing), Acta Mater., Vol. 52, 2004, pp. 2461-2474.

REFERENCES

[1] I. Etsion, O. Levinson, G. Halperin, and M. Varenberg, Experimental Investigation of the Elastic-Plastic Contact Area and Static Friction of Sphere on Flat, ASME J. Tribol., Vol. 127, 2005, pp. 47-50.
 [2]C. H. Lee, and A. A. Polycarpou, Static Friction Experiments and Verification of an Improved Elastic-Plastic Model Including Roughness Effects, ASME, Vol. 129, 2007, pp. 754-760